THE HYSICS POINTING SYSTEM: A TWO-AXIS GIMBAL MOUNTED TO THE ISS

Rick Rainy [(1)], Ryan Bolin [(1)], Patrick Brown [(1)], Ryan Lewis [(1)]

[(1)] Laboratory for Atmospheric and Space Physics,
1234 Innovation Dr, Boulder CO 80303, USA

ABSTRACT

The CLARREO (Climate Absolute Radiance and Refractivity Observatory) Pathfinder (CPF) mission will measure Earth-reflected sunlight with unparalleled accuracy over existing reflected solar (RS) sensors and will also serve as an on-orbit inter-calibration reference to other orbiting sensors. In order to achieve these goals, the HySICS (HyperSpectral Imager for Climate Science) instrument will need to be pointed at a diverse set of targets including: nadir earth, co-aligned earth scans with other orbiting sensors, the Sun, and the Moon. These pointing targets necessitate a large range of angular motion with high pointing accuracy and a wide range of variable scan rates. To meet these challenges, a unique 2-axis gimbal mechanism was developed along with associated mechanical structure and launch lock mechanisms. Taken together, these mechanisms form the heart of the HySICS Pointing System (HPS) that will be described in this paper.

After the CLARREO Pathfinder system is mounted on the International Space Station (ISS), three launch lock assemblies will deploy, and the HPS will provide on-orbit pointing control for the instrument. This paper discusses the mechanical design drivers that led to the flight gimbal's unique architecture, including custom brushless DC (BLDC) actuators, flexible harnessing, and shape-memory alloy release mechanisms.

The paper will also discuss several lessons learned during the development, assembly, and testing of the HPS. The authors have also re-evaluated the overall cradle architecture after several anomalies unexpectedly required the complete disassembly and reassembly of the HPS.

1 MISSION INTRODUCTION

The CLARREO Pathfinder payload will be externally mounted to the International Space Station (ISS) as soon as 2025 for a 1-year prime mission. CPF is led and managed by the NASA Langley Research Center (LaRC), while the majority of the payload implementation is the responsibility of the Laboratory for Atmospheric and Space Physics (LASP) at the University of Colorado, Boulder.

The heart of the payload is the HySICS instrument, a hyperspectral imager that was developed by LASP as part of a NASA instrument incubator program (IIP) starting in 2007 that culminated with proof-of-concept flights on high altitude balloons in 2013 and 2014 [1]. HySICS measurements are achieved in push-broom fashion with a 70-km cross-track swath width at nadir and 350-2300 nm spectral range. The HySICS radiometric accuracy is up to an order of magnitude better than existing on-orbit instruments, which is achieved by regularly calibrating against the Sun.

The CLARREO Pathfinder mission will leverage the increased HySICS accuracy to achieve several important scientific goals. First, it will provide high accuracy measurements of Earth-reflected sunlight across a broad spectral range that will provide critical insights into the Earth's changing climate. Second, CPF will serve as an on-orbit reference to help calibrate existing orbiting sensors. Third, CPF will measure the reflected radiance of the Moon, which will greatly improve the Moon's usefulness as a vicarious calibration target for other sensors.

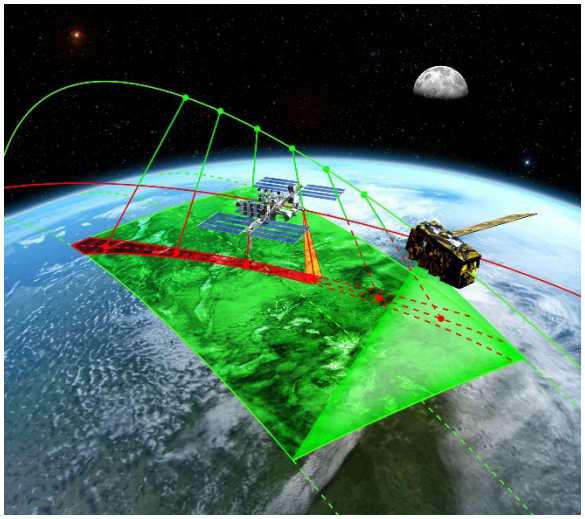

Figure 1: Orbit track of CPF on ISS (red) crossing under the Suomi-NPP or NOAA-20 orbit track (green), which demonstrates the ability of CPF to match elevation and azimuth angle of inter-calibration targets (CERES or VIIRS). (Courtesy NASA)

To support these scientific objectives, the HySICS instrument needs to be pointed at a wide variety of targets, which led to the need for the HySICS Pointing System (HPS). These targets include: nadir earth, earth

ground targets, co-aligned earth scans with other orbiting sensors (Fig. 1 above), the Moon, and the Sun.

After launch in the trunk of a Dragon capsule of a Falcon 9 rocket, CPF will be installed onto external Site 3 of Express Logistics Carrier-1 (ELC-1) (Fig. 2 below), which is on the outboard (port), forward (ram) and nadir (earth) sides of the ELC. Although this location is well-suited to view its targets, the large, complex structure of the ISS ultimately limits the useful field of regard (FOR) for CPF. Given these obscuration constraints and the nominal line of sights to the Earth, the Moon, and the Sun, a large range of angular motion was specified for the HPS that allows for viewing most of the Earth disk and the Moon and the Sun after sunrise in the forward direction. The scan motions that co-align the HySICS with other instruments' lines of sight and that provide scanning across the Moon and Sun require that the HPS be capable of scanning at variable rates (0.07 to 2 deg/sec), with sub-arcminute pointing accuracy, and jitter less than 15 arcsec (k=1). Additionally, observations of the Earth must be geolocated to within 250 m (k=1) at nadir.

The combination of these mission requirements led to the development of the HPS with a broad set of pointing capabilities and medium-high pointing performance.

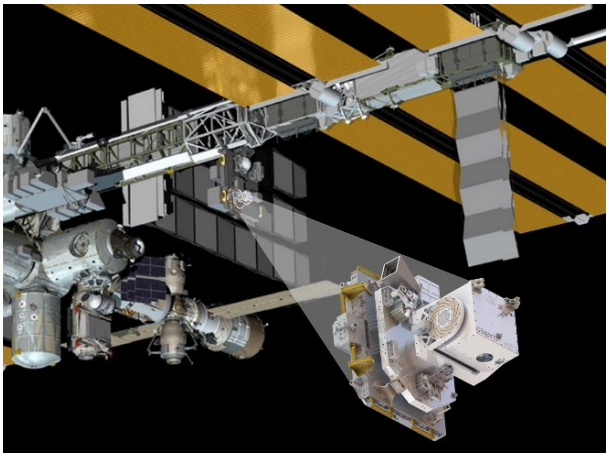

Figure 2: CPF Mounting Location on the ISS ELC1-3

2 HARDWARE DESCRIPTION

2.1 Payload Overview

The CPF payload (Fig. 3 below), consists of many components, several of which will be described in more detail below.

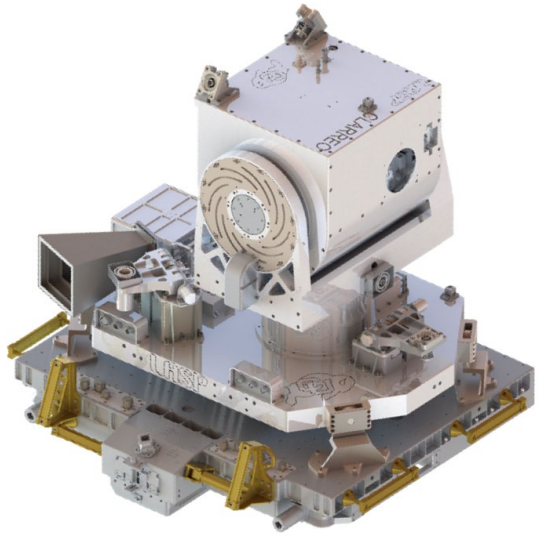

Figure 3: CLARREO Pathfinder Payload

Starting at the interface to the ISS is the ISS-provided Express Pallet Adapter (ExPA), which also provides an interface for installation into the Dragon trunk for launch., The ExPA also provides the attachment for the payload to be robotically installed onto the ISS ELC. Two CPF components mount to the ExPA—the baseplate is attached to the ExPA via four flexures, and the LaRC-provided Power Conversion Unit (PCU) is bolted directly to the ExPA under the baseplate. The baseplate houses several components, including the HPS gimbal system, the launch locks, the HPS Controller (HPSC) electronics box, the microASC star tracker from Technical University of Denmark (DTU), and wire harnesses. Within the gimballed cradle structure resides the HySICS instrument, the High-rate Fine Sun Sensor (HFSS), which is attached directly to the HySICS enclosure, the HySICS Instrument-Spacecraft Interface Electronics (HISIE) box, the cryo-cooler, the cryo-cooler electronics, and wire harnesses.

The CPF payload (without ExPA) weighs approximately 270 kg, and is roughly 1.2 x 0.9 x 1.0 m (L x W x H) in size.

2.2 Comparison to TSIS

The CPF payload borrows many design and hardware elements from the TSIS-1 payload that is also mounted on the ISS [2][3]. Overall the two payloads are approximately the same overall volume and mass. The CPF payload reuses the TSIS-1 main baseplate assembly, including the four titanium flexures. The HPSC electronics box is a rebuild of the TSIS-1 ISIE electronics box, and the HPSC is mounted in the same location as the TSIS-ISIE. Both payloads also utilize 2-axis brushless-DC (BLDC) gimbals that are mounted to the baseplate to point their scientific instruments.

Unlike TSIS-1, the Third Axis Deployment system (TADS) was not needed for CPF, because it has less stringent FOR requirements. The TSIS-1 TADS design allowed the payload to fit into the stowed envelope in the Dragon and then deploy on-orbit to achieve the necessary viewing angles. Because CPF does not include the TADS, it was necessary to develop a different launch lock system for the instrument. For TSIS-1, the launch locks were fixed and the instrument, via the TADS, moved away from the restraint system. For CPF, the launch locks, when released, rotate away from the instrument. For TSIS-1, which had two instruments, those instruments were mounted to a large common plate, with the instruments only being covered by MLI. For CPF, the HySICS instrument is mounted inside the cradle and is fully enclosed by metal plates.

2.3 Baseplate

The CPF payload base structure consists of a large 3-inch thick lightweighted aluminium plate that mounts to the ExPA via four titanium flexures. Each flexure has a spherical bearing pressed into one end, which is slid into a clevis and inserted onto a large stainless steel dowel pin. The flexure base mounts to the ExPA's ¼-28 hole pattern, and also utilizes the ExPA's shear puck accommodation at each flexure.

The HPSC is mounted to the baseplate and provides control of the BLDC actuators, control of the launch locks, and serial/power interfaces to the HISIE, the HFSS, and the star tracker. To reduce excessive displacements and stresses seen by the HPSC during initial structural analysis, an additional structural interface was added under HPSC between the baseplate and the ExPA. This small "tension link" uses dual spherical bearings and pins to ensure a purely axial load with no moment transfer.

The microASC star tracker is directly mounted to the baseplate via a custom bracket on titanium flexures. The star tracker provides direction measurements of the CPF baseplate attitude in inertial space to aid in meeting the geolocation requirement. The star tracker baffle is laminate carbon fibre, and the bracket includes a small radiator area for radiating heat away from the camera head unit (CHU) to deep space. The star tracker Data Processing Unit (DPU) electronics box is also mounted to the baseplate and serves as the electrical interface between the HPSC and the CHU.

In the launch configuration, the HPS gimbal is secured to the baseplate via three launch locks. Further descriptions of the gimbal and the launch locks are provided in sections below.

2.4 Gimbal

The primary component of the HPS is the 2-axis elevation-over-azimuth gimbal that includes three subassemblies: the azimuth assembly (aka azimuth pedestal), the yoke assembly, and the cradle assembly (Fig. 4 below). The azimuth assembly is the structure for the azimuth actuator and houses the "omega flex" chamber for the flex harnesses routed from the baseplate to the yoke. The yoke assembly has a base and two sides, with one side supporting the elevation actuator, and the opposite side containing the omega flex chamber for a second set of flex harnesses routed from the yoke base into the cradle. The second side with the flex harnesses also has a large radial bearing. The cradle assembly is a structure exoskeleton of lightweighted aluminum plates (with hatches for access) that houses the HySICS instrument within, along with additional electrical flight hardware.

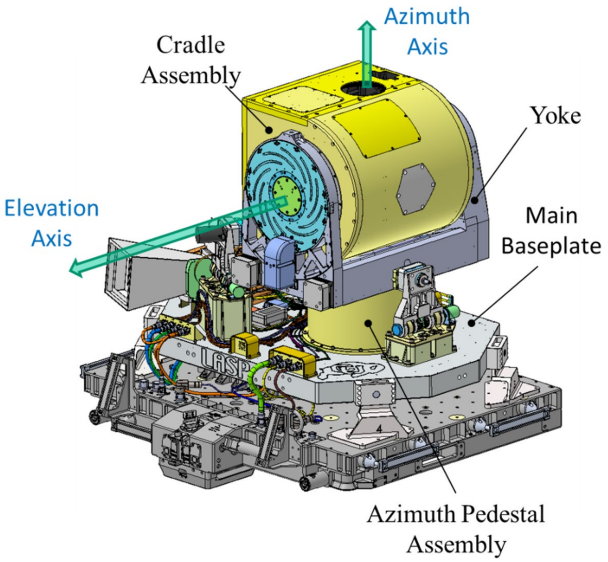

Figure 4: HPS Assembly and Pointing Directions

The azimuth axis is aligned along the ISS Y-axis (pitch) with 90 degrees of motion in the aft direction for Earth coverage and 160 degrees of motion in the forward direction for viewing of the Earth, Moon, and Sun. The elevation axis is aligned with the ISS X-axis (roll) when the azimuth axis is at its zero (nadir-pointed) position. It has 45 degrees of inboard motion before the HySICS field of view (FOV) is obscured by the baseplate structure and 90 degrees of outboard motion. Because of the restricted elevation range of motion, full Earth coverage is not within the FOR; but the available FOR is sufficient for CPF to view all its targets with ample duration and viewing frequency.

To achieve the required pointing accuracy, jitter, pointing knowledge, and scan rates, the HPS gimbal uses Moog BLDC actuators on both axes that have heritage from the TSIS-1 Thermal Pointing System (TPS) actuators. The

actuators consist of the following key components: 3-phase direct-drive BLDC motors, 2-speed (1x, 16x) resolvers, output duplex pair bearings, and housings. This design is identical to the TSIS-1 BLDC actuators, except that the brakes and twist caps were removed from the design for CPF. Based on experiences from TSIS-1 and discussions with ISS engineers, it was determined that brakes were not required to meet requirements during end of life translation by the robotic arm into the Dragon trunk. The decision to not incorporate twist caps will be discussed in their own section below.

The BLDC actuator bearings are the same configuration as the set used for TSIS-1 and consist of a large, 5.5 inch OD, thin section, duplex pair mounted in a back-to-back configuration. The set is hard preloaded and is designed to adhere to a maximum on-orbit Hertzian contact stress (HCS) of less than 120 ksi mean. The duplex bearings are large enough that the launch HCS values for CPF are well below the quiet running torque of 335 ksi mean.

The elevation axis includes a secondary, radial contact bearing on the opposite side of the yoke from the BLDC actuator that helps to support the large moment load produced by the cradle assembly. The radial contact bearing is mounted in a flexure system that allows for a minimal amount of radial misalignment. Preload for the radial bearing is low at approximately 10 lbs axially.

Both the duplex pair and the radial bearing are lubricated with Braycote 815Z oil, which is the same oil that was used successfully for TSIS-1. The material used for all bearings, both races and balls, is 440C stainless steel with phenolic ball retainers.

2.5 Flex Harnesses

The CPF design does not use twist caps to carry signals and power across the gimbal axes for two main reasons. First, the heritage twist caps would have extended the overall length of the BLDC actuators in directions that would have caused CPF to exceed its allowable volume requirements. And second, decoupling the flex harness from the actuators allowed the accommodation, fabrication, and analysis of the flex harnesses to occur in parallel with that work for the BLDC actuators.

For these reasons, flat flex harnesses were incorporated early into the design. Instead of a bundle of wires, these harnesses have copper traces in a Kapton substrate, soldered at each end to connectors. The flat pattern for these harnesses resemble the shape of the Greek letter omega (Ω), so they were labelled “omega flex harnesses.” The harnesses are split up into two groups: azimuth (rotating about the azimuth axis within the azimuth pedestal) and elevation (rotating about the elevation axis within the radial bearing side of the yoke). In these two areas, the harnesses are routed within a dedicated “omega chamber” where the harness can bend back onto itself as the HPS gimbal rotates. The harnesses are attached to both the stationary side and the rotating plate (attached to the actuator output interface) via fastened clamps with Viton gaskets. These clamps allow for a small amount of freedom for the harness to slide through the clamp as the structure is assembled, but they keep the harness restrained radially when the assembly rotates. The harnesses in each group are stacked up, with several ribbons of harness in each group; some of these harnesses have more than one layer per harness.

Because the flex harnesses were a new design, a life test was conducted, but the initial flex harness design failed its life test shortly after the test began, about 10% into the planned 30,000 cycles. After extensive investigation into the cause of the failure, it was determined that cracks were found within the copper traces in “regions experiencing high cyclic stresses and strains during testing.” [4] The flex harnesses were subsequently redesigned and fabricated to mitigate these issues, and a second life test was successfully performed prior to installation of the flexes into the flight HPS assembly.

Following installation, it was discovered that the redesigned flex allowed for cross-coupling of noise between the elevation motor signals and the elevation resolver signals. The magnitude of this noise was sufficiently large to prevent the HPS from meeting its pointing jitter requirements. The root cause of the issue was that a shield layer was not included in the new design. The flight spare harness was reworked to include a shield layer in the appropriate location, and initial bench level testing showed that this fix fully resolved the issue. For the flight assembly, the HPS was disassembled and reassembled to include this newly modified flight harness, and testing showed that the issue was fully resolved.

This second issue with the flex harnesses revealed a lesson learned: particular attention is required to prevent electrical interference between layers, both in initial design and when re-evaluating a defective design. The geometry of the traces in the stacked ribbons did not require the shield layer in the original design, but the design change to resolve the failed life test issue changed that geometry enough that a shield layer was required.

2.6 Launch Lock Design

Launch lock assemblies were incorporated into the design to secure the otherwise freely moving gimbal during launch and provide a structural load path to the baseplate. The launch locks need to disengage from the gimbal after CPF is installed onto its location on the ISS, and then they need to move out of the way of the rotating

gimbal by swinging down toward the baseplate. To satisfy these requirements, the launch lock design has two mission critical mechanisms: the hold down and release mechanism (HDRM), and the hinge line joint.

The HDRM mechanism within each launch lock utilizes an off-the-shelf EBAD TiNi Ejector Release Mechanism (ERM) . Each ERM is rated for 4000 lbs of pre-load via a 3/8-24 restraint bolt. The launch locks were designed for two configurations: with or without the ERM in the hinge. The difference in the configurations is due to design limitations preventing access to the restraint bolt during reset and pre-load in the three locations that the launch locks are placed, roughly 120° apart around the azimuth axis of the gimbal. Two of these launch locks interface directly with the cradle, and the third launch lock interfaces with the yoke.

Preload through the ERM joint was measured using a Strainsert load indicator from a strain gage internal to each custom restraint bolt. The final preload value of 3500 lbf was selected to ensure sufficient margin relative to structural analysis results and to account for small amounts of preload loss due to settling that could occur during ground operations, such as transportation events or vibration testing. Comparing preload values before and after vibration testing, including two short transportation events, the restraint bolts saw 4-7% pre-load loss.

The hinge assemblies of the launch locks contain a series of roller bearings and Vespel bushings. Radial needle bearings are located at the interface between the stainless steel shaft and the launch lock base bracket. The shaft is inserted through Vespel bushings in the hinge bracket. Needle thrust bearings are located at the axial interface between the base and hinge brackets. Torque is provided by two torsion springs, each providing 16 in-lb/rev. To reduce impact shock and for human safety reasons, a viscous damper made by DEB reduces the rate of rotation (3 in-oz max). Deployment from ERM actuation to impact with the Viton O-ring bumpers in ambient conditions is approximately 0.5 seconds.

At the separation interface where the ERM actuates, the two contacting surfaces are dissimilar materials to prevent cold welding and stiction: a “sphere” made of Nitronic 60 contacts a “cup” made of Stellite 6B. The sphere has a diameter of approximately 2.25 inch, making contact with a 60 degree surface on the cup.

Once fully assembled onto the baseplate with the HPS assembly, it was believed that the launch locks would be in an over-constrained condition, since there are three launch locks restraining 2 degrees of motion, with each one precisely match-machined/match-drilled/shimmed to its installation location. However, once assembled in the full HPS assembly, a small amount of axial play was measured, approximately 0.007 inch total (± 0.0035 inch). The launch locks’ hinge lines are roughly tangent to that azimuth rotational circle, and it was about that azimuth axis that the launch locks were able to move slightly, which was documented as an anomaly that needed resolution.

Even in this anomalous state, the launch locks were first shown to successfully actuate and deploy. To fix the axial play issue, the launch locks were removed from the HPS assembly. The axial play in each assembly was measured using feeler gauges, and then each one was disassembled by removing the hinge bracket from the base. Stainless steel shims were cut to match the interface area of the thrust bearings on the base bracket, and the shims were installed at that interface, followed by full re-assembly of each launch lock and re-installation into the HPS assembly. The axial play in each launch lock measured to be about 0.022 inch before shimming, and about 0.004 inch after shimming. Once fully reassembled, the total axial play of the full HPS assembly was re-measured to be less than 0.001 inch.

2.7 Structural Analysis and Testing

The CPF payload design was greatly influenced by three driving requirements: the launch loads, the stowed fundamental frequency, and the on-orbit fundamental frequency. Adjustments and changes to the CPF payload design were made based on the results from the structural analysis. For instance, the initial launch lock design was abandoned after analysis indicated that the stowed fundamental frequency wouldn’t meet the stowed frequency requirement of 35 Hz. Structural analysis also indicated that the TSIS-1 flexure design that CPF was using needed to be modified to handle the new loads and CG difference between TSIS-1 and CPF. In addition to analysis, multiple tests were performed on the CPF payload.

Modal testing was used to validate the structural analysis results prior to subjecting the CPF instrument to the planned structural verification test (SVT). Modal testing was also used to validate the analysis results for the deployed on-orbit frequency and mode shape results. Results for the modal testing compared well to the structural analysis predictions. The finite element model (FEM) was then correlated to the results of the modal test.

The SVT was performed to verify the strength of the CPF payload through sine burst vibration testing. While at the vibration testing facility, random vibration testing was also performed to look at the response of both the structure and components within the HPS. For the SVT, mass models were used in place of the flight components, and force transducers were used to limit the injected loads to the appropriate levels. A system-level force-limited random vibration test is planned for CPF. This test,

however, will not include the ExPA. Therefore, only structural analysis will be used to determine launch loads and responses of the CPF payload when mounted to the ExPA. Following the system-level random vibration testing, a second model correlation will occur to support delivery of the final CPF FEM to SpaceX for the final coupled loads analysis.

During the SVT, the test levels were sequentially increased in 3 dB increments from -15 dB up to full level (0 dB). Acceleration responses typically increase linearly between levels; however, the HPS responded nonlinearly between test levels. The nonlinear responses are attributed to two HPS features. First, the HPS contains spherical bearings in multiple places, including the flexure mounts to the main baseplate and within each launch lock ERM. Spherical bearings are well known to produce the type of nonlinear responses observed during the SVT. Second, the axial play in the launch locks was never fully removed, allowing for nonlinear stiffness in that joint. Regardless of the source of the nonlinearity, the assembly as a whole settled to a steady state and correlated well with the predicted modal analysis results at full level.

3 INTEGRATION

As discussed in section 2.5 above, a large focus of the HPS design was on flex harness integration and accommodation of the HySICS instrument within the cradle, leading to an "exoskeleton" design where the flex harnesses are in internal chambers and the HySICS instrument and associated components are mounted to the interior wall of the cradle. Mechanical installation of this exoskeleton design was challenging to the point that it was commonly described as "building a ship in a bottle."

The baselined assembly, integration, and test schedule for the HPS included several disassembly and re-assembly cycles to accommodate fit check and match drilling operations, and the installation and removal of mass models for SVT. The replacement of mass models for flight hardware required the complete disassembly of the HPS cradle and half of the yoke, including the complete removal of the elevation flex harnesses. The additional anomalies associated with the flex harnesses and other schedule delays by the HySICS instrument required additional disassembly and reassembly cycles of the entire HPS assembly. Each assembly cycle required multiple overhead crane lifts that used custom lift fixtures and handling fixtures. Combining those overall handling risks with the fragile nature of the flex harnesses, which are prone to damage when handling, presented the program with additional risk in an area that had already seen many anomalies.

Throughout the HPS design and build lifecycles, it was well known that the installation and integration of the flex harness and payloads within the cradle would be a difficult and tedious operation, presenting risks to damaging flight hardware. The program schedule eventually accommodated multiple re-builds due to other issues within the program, but the handling risk associated with these cycles was due to the initial exoskeleton design. These risks were considered acceptable because the mechanical assembler team assigned to the project was very capable at performing and re-performing these assembly tasks.

Based on these experiences, it is not recommended to use this exoskeleton design approach (aka "ship in a bottle") for future programs. The schedule impacts and technical risks associated with this exoskeleton design approach may not be so easily accommodated in future programs, which might have similar or entirely different issues that require multiple additional assembly cycles beyond those in the baseline schedule. Allowing the flex harness to be easily removed and replaced without so much structural disassembly should be prioritized in future similar programs. Additionally, the scientific instrument and associated components should be more easily removed and replaced without disassembly of so much structure and without needing to crane lift the entire assembly to special handling fixtures. The design should also allow assemblers easy access for installation of harness and other electrical equipment. If further outer structure is required, either for flight load paths, for thermal reasons, to baffle the instrument, or for ISS astronaut safety, the use of shells that go around the payload could be added after installation is complete to accommodate those requirements in separate pieces of flight hardware.

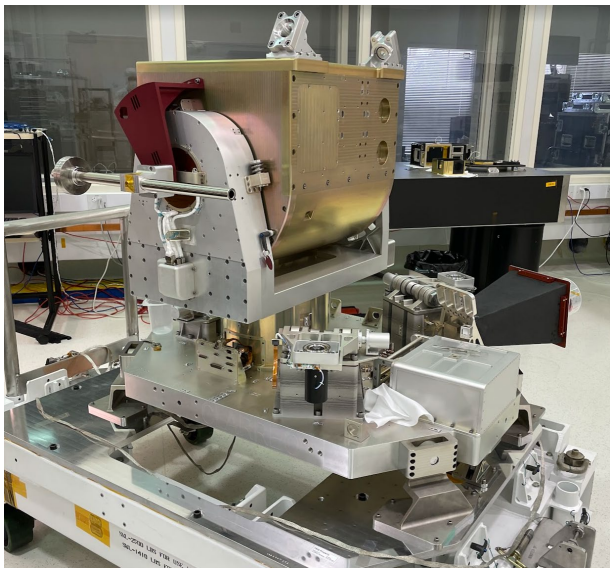

Figure 5: Fully Assembled HPS during Pointing Testing

4 TEST & VERIFICATION

4.1 Gimbal Testing

The test and verification program for the HPS gimbal control was based heavily on the TSIS-1 TPS test program and was developed to verify both functionality and performance.

Functional testing was performed after initial assembly of the gimbal (Fig. 5 above) and after every significant configuration change. Functional testing verified: the phasing, continuity, and range of the resolver angles; the phasing and response of the current controllers; the closed-loop step response behaviour; and the response of constant-rate slews over the full range of motion. The range-of-motion scans provided a consistent method to estimate the internal losses of the gimbal actuators (i.e., bearing friction, flex torque, etc), and these measurements were trended over the course of the test program to verify acceptable torque margins and performance stability.

Performance testing consisted of several key types of testing: resolver calibrations, frequency response measurements, rate characterizations, and solar testing.

Accurate calibration of the resolvers was necessary to meet the geolocation requirement of 250 m (k=1) nadir equivalent. To calibrate the resolver angles, a special test stand was developed to mount each actuator to a non-flight optical encoder that served as the absolute reference. Resolver angles were then compared to encoder angles to develop linear and nonlinear corrections that were applicable over the full operational temperature range and that allow the resolvers to support geolocation with sufficient accuracy.

Frequency response testing is another cornerstone of the gimbal controller test program that was leveraged heavily on the TSIS-1 TPS [5][6]. Frequency response measurements accomplished several goals: identification of key system dynamics (e.g., inertia, structural modes), tuning of the closed-loop control response in the frequency domain, and direct measurements of controller stability (i.e., gain, phase, bending margins). Similar to the functional tests, the frequency response measurements were performed after every significant configuration change.

Although the frequency response measurements were a necessary component in the tuning process, they were not sufficient on their own to evaluate performance versus pointing requirements. To evaluate the effect of self-induced jitter, rate characterization tests were performed that evaluated tracking errors in the time domain at various slew speeds compared to jitter requirements. If the resultant jitter did not meet requirements, the controller was retuned in the frequency domain and then rate characterization tests were performed again in the time domain. This tuning approach was performed until tracking jitters were sufficiently low to meet pointing requirements.

The final set of gimbal controller performance tests were conducted to measure performance of the solar controller that uses the HFSS [3] for feedback control. These tests included additional frequency response measurements/tuning and closed-loop control tests with a simulated stationary solar stimulus while the gimbal was mounted to a single-axis rotation stage in the same manner that the TSIS-1 TPS was tested [2][6].

Finally, after all of the functional and performance tests of the gimbal were complete, the HPS was used to support testing of the various HPS algorithms that point the HySICS instrument at the Earth, co-aligned targets with other sensors, the Sun, and the Moon.

4.2 Launch Lock Testing

The launch lock design was considered a high risk area of the program, since the use of ERMs and the overall hinging launch lock design was new for CPRS compared to previous programs at LASP (even if many of the piece parts and materials had been similarly used). For these reasons, a test program was performed on an engineering model (EM) version of one of the launch lock assemblies to help prove out manufacturability and to verify performance. The EM launch lock assembly consisted of a flight launch lock hinge assembly in a non-flight structure resembling the geometry of the flight hardware structure. The EM test campaign actuated the launch lock's ERM on both primary and secondary circuits over a range of expected flight-like environments.

The EM was initially actuated twice on the bench in ambient conditions, including instrumenting the assembly with shock accelerometers to measure the shock SRS profile of the actuation. These shock tests revealed three shock events in each actuation: the ERM actuation itself, followed quickly by the restraint bolt contacting the inside of the structure that captures it, and then the hinge assembly contacting the bumper stops. All events were very low shock, but the restraint bolt contacting its capturing structure was the largest shock event, since it was metal on metal. The measured shock environments were lower than initially anticipated, and are low when compared to GEVS "benign" curves for standard electronics. In terms of performance, the launch lock assembly performed as expected without any issues.

The EM assembly was then tested in a thermal vacuum (TVAC) chamber under both hot and cold extreme temperatures, again without any issues. The deployment time increased under hot conditions and decreased under cold conditions due to the viscous damper. The assembly

was then thermal cycled to hot and cold extremes four times before a final TVAC deployment. The assembly was then removed from the test chamber and actuated two more times in ambient conditions, again with shock accelerometers, and no noticeable changes were noted in its performance. The test campaign was successful, with no anomalies, which proved that the mechanical and electrical design of the launch locks was sound.

After the HPS subsystem was fully assembled, the flight model launch locks were tested several times. Initial tests were performed to verify end-to-end functionality with the HPSC flight electronics, the flight software, and the ground software. During these tests, the ERM actuation pulse duration had to be increased to provide reliable separation under all conditions, but otherwise the testing proceeded nominally. Additionally as previously described, the launch locks were successfully tested following the SVT, which was the most stressing and flight-like scenario in which they have been tested.

4.3 Remaining Work

The next phase for the CPF program will be the integration and test (I&T) phase for the full CPF system that includes the HySICS instrument and its associated hardware components (HISIE electronics box, cryocooler, cryocooler electronics, and harnesses) installed into the cradle. This phase will include a full suite of functional (Aliveness, Limited Performance Test, Comprehensive Performance Test) and environmental (vibration, TVAC, EMI/EMC) tests, some of which will include the payload installed onto the flight ExPA.

After system-level I&T is complete, CPF will go into storage at LASP for approximately one year while awaiting its official manifest to the ISS. During this storage period, the CPF payload will undergo periodic testing to verify continued functionality and to exercise all mechanisms to reduce lubricant pooling within bearings.

After a manifest has been established, CPF will be shipped to Kennedy Space Center for final interface testing, integration into the Dragon trunk, and launch on a Falcon 9 to the ISS. After arrival to the ISS, CPF will be robotically installed on Site 3 of ELC-1 followed by 60 days of commissioning activities. Finally, CPF will commence measurements for its one year mission.

5 ACKNOWLEDGEMENTS

The authors would first like to thank our partners at the NASA Langley Research Center for their unwavering support, direction, and sponsorship of CPF.

We would also like to acknowledge and thank all of our LASP colleagues who we have worked with to make CPF a reality. In particular, much of the credit for the HPS design belongs to Kraig Koski. We also owe gratitude to Tim Holden, the CPF lead systems engineer, for his technical direction and guidance. Finally, we would like to thank Greg Ucker, the LASP project manager for CPF, for his ongoing support of the HPS.

6 CONCLUSIONS

The CPF HPS has been designed, built, and tested to provide precise pointing of the HySICS instrument at a diverse set of targets over a wide angular range from its site on the ISS. The design leveraged several key features from the TSIS-1 pointing system, while also tailoring specific design facets to the CPF mission. Generally, the HPS has successfully met all its requirements, but two design aspects (omega flexes, exoskeleton) presented challenges that led the authors to reconsider those choices for future projects. The HPS is ready for system-level integration and test and eventually for on-orbit operations.

7 REFERENCES

1. Kopp. G., et al., “Radiometric flight results from the HyperSpectral Imager for Climate Science (HySICS)”, *Geoscientific Instrumentation Methods and Data Systems, 2017*

2. Brown, P., Engelmann, A., & Lewis, R., “Use and Advantages of Direct-Drive Brushless DC Actuators for Precision Instrument Pointing of the Total and Spectral Solar Irradiance Sensor”, *Proceedings of the 44th Aerospace Mechanisms Symposium, May 2018.*

3. Brown, P., “Challenges and Solutions for Precision Solar Pointing on the ISS for the TSIS Instrument”, *Proceedings from the 2019 IEEE Aerospace Conference.*

4. Sood, B., et al., “Analysis of a Dynamic Flexed Flat Cable Harness”, *Proceedings from IPC APEX EXPO, 2022.*

5. Engelmann, A., “Modeling, Simulation, and Robust Design of the TSIS Pointing Controller for ISS Deployment”, *Proceedings from the 2019 IEEE Aerospace Conference.*

6. Brown, P., Engelmann, A., “TSIS Experiences with ISS Jitter from Inception to On-Orbit Operation”, *Proceedings from the 42nd American Astronautical Society Guidance, Navigation, and Control Conference, February 2019.*